Nature of surface deposits on sulfated zirconia used as catalyst in the benzoylation of anisole

A. Trunschke [a,*], J. Deutsch [a], D. Müller [a], H. Lieske [a], V. Quaschning [b] and E. Kemnitz [b]

[a] *Institute for Applied Chemistry Berlin-Adlershof, Richard-Willstätter-Str. 12, 12489 Berlin, Germany*
[b] *Humboldt University, Brook-Taylor-Str. 2, 12489 Berlin*

Received 6 June 2002; accepted 11 July 2002

The benzoylation of anisole with benzoic anhydride over sulfated zirconia has been investigated, especially with regard to catalyst deactivation and regeneration. Calcined sulfated zirconia and spent catalysts have been characterized by BET analysis, C–H elemental analysis, DRIFTS, NH_3-TPD, ^{13}C-NMR and UV–Vis spectroscopy. In batch-mode experiments, a moderate deactivation attributed to the deposition of carbonaceous surface species has been observed. The surface deposits consist of benzoate species and strongly adsorbed molecules of anisole. A color change of the solid, observed immediately after the introduction of the catalyst into the reaction mixture, has been attributed to the protonation of the reaction products 2- and/or 4-methoxybenzophenone. The surface species formed may cover or modify surface acid sites and, in this way, reduce the accessibility of active centers. Removing the deposited and adsorbed species by calcination in air restores the initial activity of sulfated zirconia.

KEY WORDS: sulfated zirconia; Friedel–Crafts acylation; benzoylation; deactivation; regeneration; anisole; benzoic anhydride; solid acid catalyst.

1. Introduction

The Friedel–Crafts acylation of aromatic ethers is widely applied in synthetic organic chemistry and the chemical industry to obtain aromatic ketones, which are valuable chemical intermediates for pharmaceuticals, speciality chemicals or fragrances. The reaction, which involves the substitution of a hydrogen atom of the aromatic substrate by an acyl group, is commonly performed in the presence of stoichiometric or even excess amounts of Lewis acids, like $AlCl_3$, or Brønsted acids, like H_2SO_4, polyphosphoric acid or HF. Prompted by environmental restrictions and the inconvenience of handling corrosive reaction media and acidic wastes, a wide range of solid acids, like perfluorinated resinsulfonic acid (Nafion-H), zeolites, mesoporous alumosilicates and sulfated metal oxides [1] as well as clays [2] or heteropolyacids [3] have been suggested to replace conventional homogeneous Friedel–Crafts acylation catalysts. Besides zeolite H-Beta [4], sulfated zirconia appeared to be the most promising solid acylation catalyst [1,5–10].

In previous works, we have studied the catalytic properties of different types of sulfated zirconia, prepared by precipitation and by sol–gel procedures in batch-mode acylations of anisole with benzoic, acetic and propionic anhydride [7,9–10]. These reactions have been applied to investigate structure–reactivity relationships in liquid-phase acylations on solid acids. Evidence was found that the coincidence of sufficiently large pore diameters and a significant number of acid sites possessing appropriate acidity are essential for high catalytic activity of sulfated zirconia in liquid-phase acylations [9]. Although the number of surface acid sites decreased during benzoylation of anisole and carbonaceous deposits were accumulated on the catalyst surface, only a moderate catalyst deactivation was observed [9]. The above experiments have motivated efforts aimed at acquiring evidence of links between decreased acidity and accumulation of deposits on the one hand and loss of catalytic activity on the other hand.

Especially in view of the industrial application of solid acid catalysts, deactivation, reusability and availability of facile regeneration procedures are subjects of importance. Nevertheless, only moderate attention has been devoted to the investigation of deactivation phenomena in liquid-phase reactions over solid acid catalysts up to now. A number of recent papers deal with deactivation of zeolites, mainly H-Beta, during Friedel–Crafts acylation reactions [11–17]. Irreversible adsorption of polar reaction products has been frequently observed [11,12,14,16]. In the acetylation of anisole by acetic anhydride, product inhibition, *i.e.,* strong adsorption of *p*-methoxyacetophenone in the mesopore volume of H-Beta, has been established by Rohan *et al.* [11]. Moreover, these authors have observed pore blockage due to accumulation of large molecules in the zeolite micropores originating from polyacetylation and consecutive reactions of polyacetylated intermediates. Acetic acid formed in acetylations by acetic anhydride has also been suggested to cause deactivation [14].

* To whom correspondence should be addressed.
E-mail: at@aca-berlin.de

1011-372X/02/1100-0271/0

The present work was undertaken to study reaction-initiated surface modification and regeneration of sulfated zirconia in the benzoylation of anisole. For this purpose, kinetic investigations in batch mode have been performed. The surface characteristics of calcined, used and regenerated catalysts have been examined by spectroscopic methods.

2. Experimental

2.1. Catalysts

Two different types of sulfated zirconia, prepared by a standard procedure, SZ(1), and by a sol–gel procedure, SZ(2), have been studied. The preparation methods have been described elsewhere [7]. Briefly, SZ(1) was made by kneading a precipitated $ZrO_2 \cdot xH_2O$ with solid $(NH_4)_2SO_4$, followed by calcination in air at 500 °C for 3 h. For comparison, precipitated S-free zirconia was calcined at the same temperature. SZ(2) was prepared from a $Zr(OPr)_4$ solution in propanol, by adding a mixture of nitric acid and sulfuric acid. Supercritical drying was carried out at 280 °C and 150 bar, and the aerogel was calcined in air at 500 °C for 3 h.

2.2. Chemicals

Anisole (99% GC) and benzoic acid carboxy-^{13}C (99 atom% ^{13}C) were purchased from Aldrich, and benzoic anhydride (97%) from Fluka. Anisole was dried and stored over sodium wire. Benzoic anhydride carboxy-^{13}C was synthesized from benzoic acid carboxy-^{13}C, according to ref. [18].

2.3. Catalyst characterization

The specific surface areas and porosities of the catalysts have been determined by nitrogen adsorption at −196 °C, using a BET area analyzer (NOVA-1200, Quantachrome Corp.). The total number of acid sites was measured using temperature-programmed desorption (TPD) of ammonia, which was adsorbed at 100 °C. The sample was purged for 30 min with He at 100 °C before starting the TPD run to remove physically adsorbed ammonia. The ammonia desorbed from the catalyst was absorbed in 0.1 N sulfuric acid and titrated. The nature of the acid sites was studied by FTIR-NH_3-TPD. The measurements were carried out on self-supporting wafers of *ca* 10–20 mg cm^{-2} in a transmission infrared quartz cell with CaF_2 windows that allow heat treatments in vacuum and gases. The samples have been pretreated *in situ* for 1 h in an O_2/He flow at 500 °C. After cooling down in vacuum, the adsorption of ammonia was performed at 100 °C by the admission of 15 mbar NH_3 and subsequent evacuation for 30 min at the same temperature to remove physically adsorbed ammonia. In order to follow the variations of the bands of adsorbed ammonia during NH_3-TPD (heating rate 10 °C min^{-1}), every 10° of infrared spectra were taken at increasing temperature from 100 °C to 500 °C using an FTS-60 A spectrometer (Bio-Rad). At a resolution of 2 cm^{-1}, 64 scans have been accumulated. The measurements were performed in difference mode, referring to spectra of the sample collected before NH_3 adsorption at the same temperature.

The nature of carbon-containing species on the catalyst surface was investigated by means of solid-state ^{13}C NMR, infrared and UV–Vis spectroscopy. The NMR spectra were recorded on a Varian Unity-plus 300 NMR spectrometer at 75.4 MHz. Magic-angle spinning (9 kHz) and cross-polarization techniques were applied using a Doty supersonic probe (∅5 mm rotors). ^{13}C-enriched starting material (benzoic anhydride carboxy-^{13}C) was used as an acylating agent, in order to obtain a better signal-to-noise ratio. Again, the infrared spectra were measured on an FTS-60 A spectrometer (Bio-Rad). The samples were placed into the reaction chamber of a modified diffuse reflectance attachment (Harrick) connected to a gas dosing line. The spectra were recorded at 25 °C at a resolution of 2 cm^{-1} accumulating 256 scans. UV–Vis spectra were collected in diffuse reflectance mode using a Lambda 18 UV–Vis spectrometer (Perkin Elmer).

2.4. Benzoylation of anisole

The catalytic experiments were carried out in a 50 ml round-bottom three-necked flask, provided with magnetic stirrer, thermometer and reflux condenser with $CaCl_2$ tube. The catalyst (0.2 g) was added to a stirred mixture of 12 ml of dried anisole, 0.1 g of benzoic acid *n*-butyl ester (internal standard for HPLC detection) and 0.00265 mol (0.6 g) of benzoic anhydride. The temperature was kept at 50 °C. After reaction times of 5, 10, 20, 30, 45, 60, 90, 120 and 180 min the reaction mixture was analyzed by means of HPLC (pump: L-6250 Merck–Hitachi, flow 1 ml/min; UV-detector L-7400 Merck–Hitachi, $\lambda = 235$ nm; column: RP-18.7 μm Merck; eluent: acetonitrile/water 60/40 v/v). The used catalysts were washed with CH_2Cl_2 before further characterization.

3. Results and discussion

3.1. Surface structure and acidity of calcined catalysts

3.1.1. DRIFTS

Especially in view of the application of SO_4-modified zirconia in acid-catalyzed gas-phase reactions, like isomerization of light alkanes, sulfated zirconia has been studied extensively in the past with respect to the

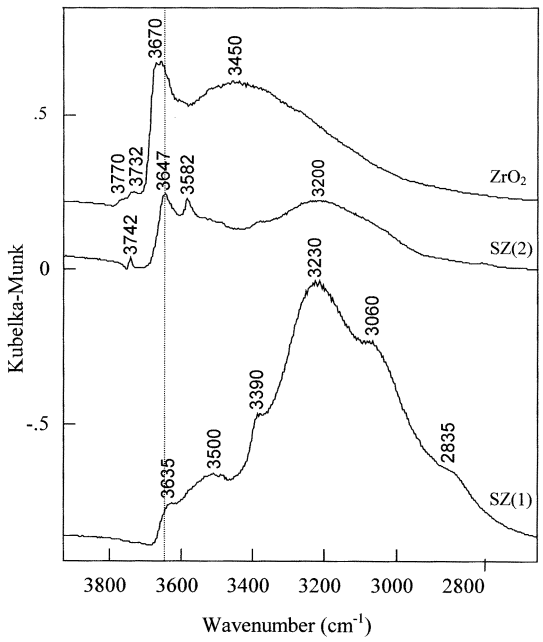

Figure 1. DRIFT spectra of SZ and ZrO_2 after calcination in air at 500 °C in the region of OH-stretching vibrations.

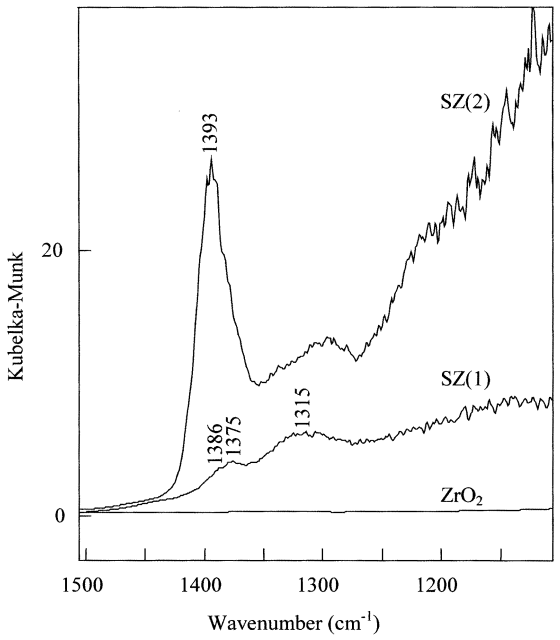

Figure 2. DRIFT spectra of SZ and ZrO_2 after calcination in air at 500 °C in the region of S=O-stretching vibrations.

molecular structure of surface sulfates and the nature of acid sites [*e.g.*, 19–31]. To characterize the surface properties of the catalysts under consideration, DRIFT spectroscopy was used.

Figure 1 displays the infrared spectra of sulfated zirconia SZ(1) and SZ(2) and the sulfate-free zirconia precursor of SZ(1) upon *in situ* calcination at 550 °C in the region of OH stretching vibrations. The DRIFT spectrum of sulfate-free ZrO_2 is common and shows a broad band around 3450 cm^{-1}, due to hydrogen-bonded surface hydroxyls and peaks at 3770 cm^{-1} (very weak) and 3670 cm^{-1}, which correspond to isolated terminal and bridging ZrOH groups, respectively [32]. The band at 3732 cm^{-1} is probably due to silanol groups, indicating silica impurities of the precursor oxide. Modification of ZrO_2 by sulfate ions results in the complex spectrum of SZ(1) (figure 1), which is, however, in general agreement with previous spectroscopic studies [26,28,29]. Accordingly, the SO_4^{2-} addition is reflected in a complete elimination of terminal ZrOH groups and a frequency shift of the band of isolated bridging ZrOH groups toward 3635 cm^{-1}. The corresponding hydroxyl species have been considered responsible for strong Brønsted acidity [26–29]. The appearance of a broad band around 3500 cm^{-1} may be explained by the presence of hydrogen-bonded hydroxyl groups on non-modified surface domains of SZ(1). The dominating broad bands at 3390 cm^{-1} and around 3230 cm^{-1} and 3060 cm^{-1} are attributed to multi-center bonded protons in surface HSO_4^- structures [26]. Compared to SZ(1), the corresponding species are less abundant on the surface of SZ(2). The spectrum of SZ(2) shows a band at 3647 cm^{-1}, assigned to acidic hydroxyl groups. Moreover, a band at 3742 cm^{-1} due to silanol groups was observed. The peak at 3582 cm^{-1} is tentatively attributed to bridging ZrOH groups on non-modified surface areas of SZ(2), which differ in their configuration from S-free zirconia.

In general, the spectra of SZ(1) and SZ(2) in the OH stretching region indicate that besides acidic ZrOH groups and protons associated with sulfur-containing surface structures, a substantial amount of non-modified, *i.e.*, non-acidic ZrOH, groups are present on the surface after sulfation. The complexity of the spectra is consistent with a considerable surface heterogeneity, especially of SZ(1).

This structural variety is also reflected in the spectral range of sulfate vibrations (figure 2). The interpretation of the DRIFT spectra in the S–O stretching region (1150–850 cm^{-1}) was not possible due to almost zero reflection. Weak peaks due to S=O stretching vibrations at 1386, 1375 and 1315 cm^{-1} and a noticeable absorption above 1400 cm^{-1} were observed on SZ(1). Similar but generally better resolved bands have been observed by many authors in the 1450–1340 cm^{-1} region [19,21,24, 28,29,31]. Jin *et al.* assigned a band at 1390 cm^{-1} to asymmetric O=S=O stretching vibrations of bidentate surface sulfate species with high covalent character [19]. IR bands at 1355 and 1370 cm^{-1} were attributed to stretching vibrations of single S=O groups in two different tridentate complexes $(ZrO)_3S{=}O$ [21]. Recently, this proposal was supported by *ab initio* calculations [33]. Polynuclear, most likely S_2O_7-type species, characterized by S=O stretching frequencies above 1400 cm^{-1}, have also been suggested in sulfated zirconia [21]. On the basis of a sharp band at 1391 cm^{-1}, Babou *et al.*

Table 1
Textural and surface properties of calcined, used and regenerated catalysts.

	Catalyst	Surface area (m^2/g)	Mean pore diameter (Å)	Number of acid sites [a] (mmol/g)	Sulfur content [b] (wt%)	Carbon content (wt%)
Calcined	SZ(1)	123	54	0.33	3.5	0
	SZ(2)	138	280	0.37	1.6	0
Used	SZ(1)	112	54	n.d.	3.53	0.84
Regenerated	SZ(1)	113	55	0.31	2.83	0

[a] NH_3-TPD.
[b] Oxidation state of S in all samples: +6 (XPS).

supposed the formation of SO_3 molecules grafted on zirconia under high dehydration conditions [29]. In general, the structure of surface sulfates strongly depends on the degree of hydration. With increasing degree of hydration, highly covalent sulfates are converted into less covalent forms and finally into ionic sulfates [34]. Considering the proposals given in the literature, the spectral features observed with SZ(1) allow one to suggest the presence of hydrogen sulfates due to the absorption around 1315 cm^{-1} and two different families of surface sulfate structures characterized by the bands at 1386 and 1375 cm^{-1}. Polynuclear species also have to be considered due to the weak absorption above 1400 cm^{-1}.

The spectrum of SZ(2) is better resolved, showing an intense peak at 1393 cm^{-1} due to S=O stretching vibrations, indicating an enhanced structural homogeneity of the sulfate species on the surface compared with SZ(1).

In summary, the DRIFT spectra of the calcined sulfated zirconia catalysts studied in the present investigation indicate that sulfur is not distributed evenly on the surface. Consequently, non-modified ZrO_2 surface domains are present and will be exposed to the reaction mixture during the benzoylation of anisole.

3.1.2. Ammonia adsorption

The total number of acid sites of the calcined catalysts determined by temperature-programmed desorption (TPD) of ammonia are summarized in table 1. Accordingly, the acidities of SZ(1) and SZ(2) do not differ substantially with respect to the probe molecule ammonia.

Infrared spectroscopy of adsorbed ammonia was used to study the nature of these acid sites. The spectra observed on SZ(2) during ammonia adsorption and temperature-programmed desorption (TPD) are shown in figure 3. Brønsted acidity of SZ(2) was proved by the appearance of a band at 1445 cm^{-1} due to asymmetric bending vibrations of adsorbed ammonium ions. In parallel, the intensity of the OH band at 3638 cm^{-1}, which corresponds to acidic hydroxyl groups, decreases. With increasing temperature, the intensity of the band at 1445 cm^{-1} decreases due to ammonia desorption and the OH band reappears. In figure 4, the differences in the integrated absorbance of the peak at 1445 cm^{-1}, measured at two consecutive temperatures, are plotted *versus* the temperature. The desorption maximum was observed at about 250 °C. The broad temperature range (100–450 °C) in which the desorption of ammonium ions occurs indicates the substantial energetic heterogeneity of the corresponding Brønsted acid sites.

As can be seen in figures 3 and 4, ammonia desorption at lower temperatures (100–350 °C) is also related to the adsorbed species responsible for the peak at 1608 cm^{-1}. A similar band was also present on pure zirconia at 1603 cm^{-1} (figure 5). The peak is assigned to the asymmetric bending vibration of NH_3 coordinatively bound to Zr^{4+} ions. The corresponding symmetric bending vibration, which is observed on ZrO_2 at 1197 cm^{-1}, is covered on SZ(2) by the stretching vibrations of the sulfate groups. Ammonia molecules coordinated to such sites were essentially desorbed at 400 °C on pure

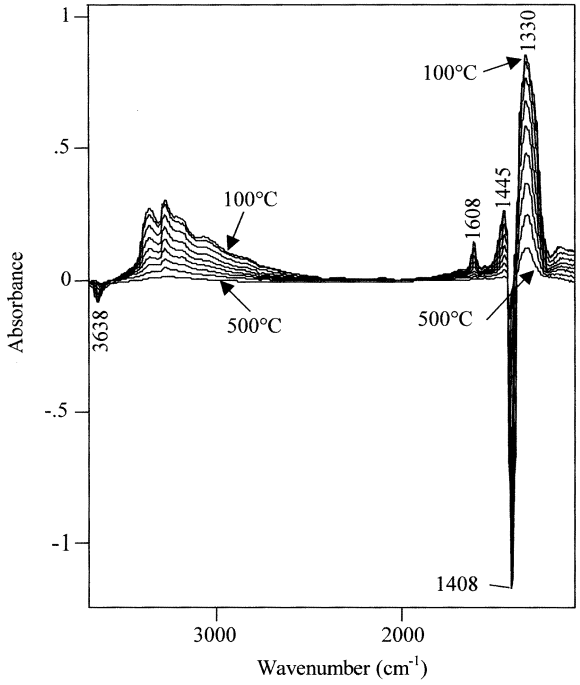

Figure 3. Infrared spectra of SZ(2) during NH_3-TPD.

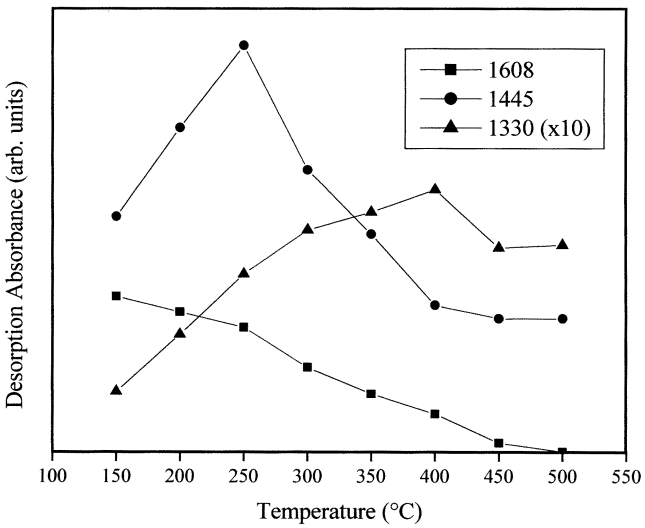

Figure 4. Desorption absorbances of the band at 1445 cm^{-1} due to ammonium ions, and the bands at 1608 and 1330 cm^{-1} due to NH_3 adsorbed on Lewis acid sites on SZ(2).

zirconia, as well as on SZ(2), pointing to comparable Lewis acidities of the corresponding Zr^{4+} ions. Therefore, the band at 1608 cm^{-1} seems to suggest the presence of non-modified surface domains on SZ(2).

Upon ammonia adsorption on SZ(2), the S=O stretching band near 1400 cm^{-1} was shifted to 1330 cm^{-1} (figure 3). This phenomenon has often been reported especially in relation with the adsorption of pyridine or ammonia, and seems to occur generally during adsorption of strong Lewis bases on sulfated zirconia [35]. In the literature, the shift of the band was explained either by an inductive effect of the Lewis base adsorbed on a Zr^{4+} ion that additionally coordinates the sulfate group [19], or by structural changes due to ligand-displacement of sulfate groups by strong Lewis bases [35]. Moreover, an adduct formation between adsorbed SO_3 and pyridine was assumed [29]. In general, the shift is related to Lewis acidity. The incomplete desorption of ammonia from the corresponding sites at temperatures as high as 500 °C indicates the presence of very strong Lewis acid centers on the surface of SZ(2).

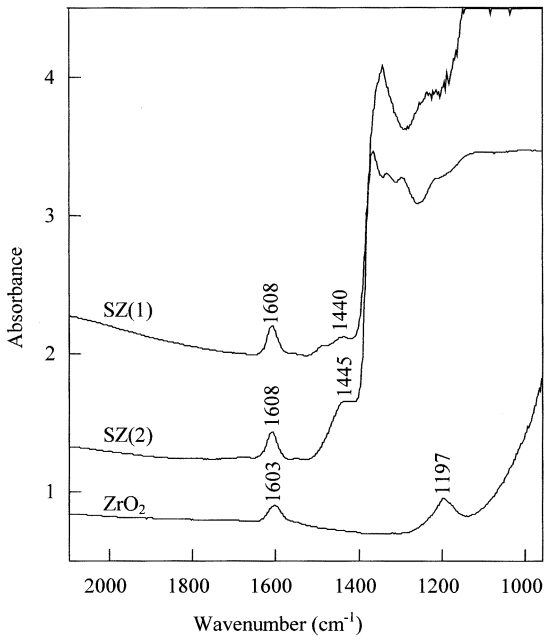

Figure 5. Infrared spectra of NH_3 adsorbed on SZ and ZrO_2 at 100 °C.

FTIR-NH_3-TPD on SZ(1) revealed similar results; however, the intensity of the band at 1440 cm^{-1} due to Brønsted acid sites was substantially lower compared with SZ(2) (figure 5). As with SZ(2), the ZrO_2 surface is partially not modified by sulfur. The ammonia desorption from strong Lewis acid sites was almost complete at 500 °C. Hence, compared to SZ(2), the strength of these sites is lower. The higher acidity of SZ(2) compared to SZ(1) found by FTIR-NH_3-TPD agrees well with the order of overall acidities established by microcalorimetric pyridine adsorption experiments in liquid phase with the same catalysts [9].

3.2. Benzoylation of anisole

The benzoylation of anisole was applied as a standard test reaction to evaluate the potential of SO_4-modified zirconia as a catalyst in liquid-phase acylation reactions of aromatics. The reaction of anisole with benzoic anhydride according to (1) gives a mixture of 4- and 2-methoxybenzophenone (MBP) (isomer ratio 96:4):

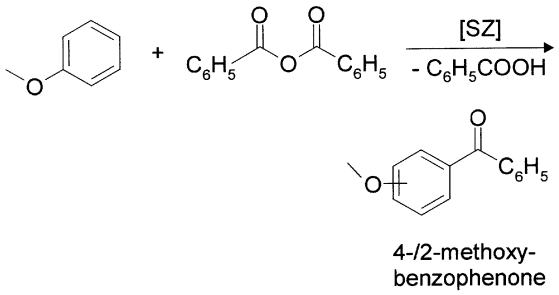

(1)

Notwithstanding the different surface characteristics, we have shown previously that the two sulfated zirconia samples are suitable catalysts for the benzoylation of anisole [7,9]. The formation of benzoic acid during the reaction is a critical point with respect to catalyst damage. To test the recyclability of sulfated zirconia, used and regenerated SZ(1) have been compared with the calcined sample. In figure 6, the yield of the ketones is shown as a function of reaction time. On the calcined catalyst, the conversion of benzoic anhydride was almost complete after 30 min. After 3 h, the catalyst was filtered from the slurry, repeatedly washed with dichloromethane, dried in vacuum (5 mbar) at 90 °C and used in a second benzoylation experiment. As becomes evident from the slope of the curves in figure 6, the used catalyst exhibited a slightly lower initial activity

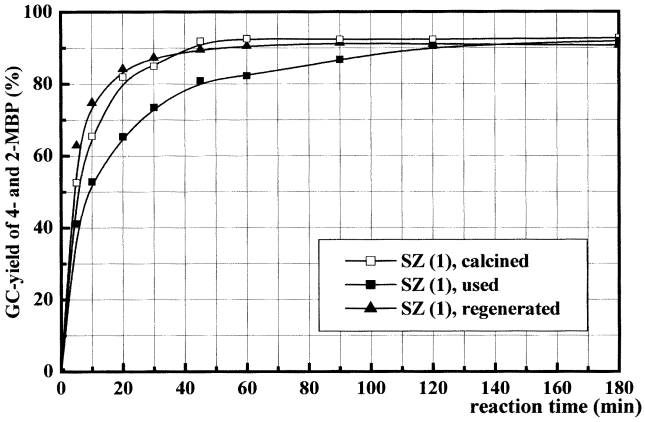

Figure 6. Kinetic studies of the formation of 4- and 2-MBP at 50 °C on SZ(1); 4-/2-MBP ratio: 96/4.

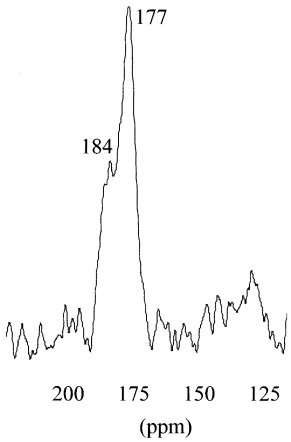

Figure 7. ^{13}C-NMR spectrum of used SZ(1).

than the calcined sample. However, the catalytic activity could be restored completely by treatment of the used catalyst in air at 550 °C for 15 min.

3.3. Texture and elemental composition of used and regenerated catalysts

A comparison of the textural and surface properties of calcined, used and regenerated SZ(1) samples is given in table 1. C–H elemental analysis revealed that carbon-containing material was deposited on the catalyst surface during reaction. The only small differences in the BET surface areas and the almost unchanged mean pore diameter of the calcined and used catalysts indicate that blockage of pores did not occur during single use of sulfated zirconia in the benzoylation of anisole. Immediately after introduction of the catalyst into the reaction mixture, the white color of the powdered sample turned into pink. The initial color could be restored and the deposited carbonaceous species could be removed completely by calcination of the used catalyst in air at 550 °C for 15 min. The combustion of carbonaceous species was coupled with a distinct sulfur loss, probably caused by the formation of volatile sulfur compounds due to the reduction of surface sulfate. According to XPS analysis, no reduced sulfur species remained on the catalyst surface after regeneration.

3.4. Surface properties of used catalysts

Applying microcalorimetry of pyridine adsorption in liquid phase at the temperature of the catalytic test reaction (70 °C), we have shown previously a decrease in the number of acid sites during benzoylation of anisole [9–10]. To examine the surface characteristics of the catalysts after reaction more thoroughly, NMR, DRIFT and UV–Vis spectroscopy were utilized.

3.4.1. ^{13}C-NMR

With the intention to identify the origin of the surface deposits, benzoylation of anisole was performed using benzoic anhydride *carboxy* ^{13}C. ^{13}C is expected to be introduced into the products 4- and 2-methoxybenzophenone. Moreover, it will be found in benzoic acid, which is formed during the reaction, and possibly in unreacted benzoic anhydride. The solid-state ^{13}C-NMR spectrum of the used, thoroughly washed and carefully dried catalyst SZ(1) shows only one distinct signal (177 ppm, 184 ppm shoulder, figure 7). For comparison, the carbonyl-group shifts of the above-mentioned carbonyl compounds [36–38] are compiled in table 2. Obviously, the detected signal is neither consistent to one of the reactants nor to an immediately formed "benzylsulfate" as a hypothetical reactive acylation agent. In view of the good correlation to the carbonyl-

Table 2
Chemical shift of the ^{13}C-carbonyl carbon in aromatic carbonyl compounds.

Aromatic carbonyl compound	Formula	Chemical shift (solvent) (ppm)	Ref.
2-Methoxybenzophenone	2-CH_3O–C_6H_4–CO–C_6H_5	196 ($CDCl_3$)	36
4-Methoxybenzophenone	4-CH_3O–C_6H_4–CO–C_6H_5	195 ($CDCl_3$)	36
Natriumbenzoate	C_6H_5–COONa	178 (D_2O)	37
Benzoic acid	C_6H_5–COOH	168 ($CDCl_3$)	37
Benzoic anhydride	C_6H_5–CO–O–CO–C_6H_5	163 ($CDCl_3$)	
Benzoyl methanesulfonate	C_6H_5–CO–O–SO_2–CH_3	162 (CD_3CN)	38

group shift of sodium benzoate, the formation of benzoate species on the catalyst surface can be taken into consideration. To elucidate the molecular structure of these carboxylate species, DRIFT spectroscopy was used.

3.4.2. DRIFTS

Figure 8 shows the DRIFT spectra of SZ(1) after calcination, and of SZ(1) and SZ(2) after use in the benzoylation of anisole. In the region of carbonyl stretching vibrations, the spectrum of SZ(1) used as a catalyst for 2.5 h at 100 °C shows bands originating from carbonaceous deposits or adsorbates at 1598, 1582, 1525, 1501, 1450 and 1425 cm^{-1}. The broad band at 1630 cm^{-1} is due to the bending vibration of molecularly adsorbed water. The water was not removed by thermal treatment to avoid destruction of the carbonaceous species under these conditions. The amount of deposits increases with reaction temperature and reaction time, as becomes obvious from the intensities of the bands due to carbonaceous residues in the spectrum of SZ(1) after use at 140 °C for 7 h. Less intense bands have been observed on SZ(2), treated under the latter reaction conditions, indicating that the amount of deposits is smaller on this catalyst.

The bands at 1525 and 1425 cm^{-1} are assigned to asymmetric and symmetric OCO stretching vibrations of bidentate benzoate species, respectively. The bands at 1582 and 1450 cm^{-1} represent the CC stretching vibrations of the benzoic ring in these benzoate complexes. Generally, surface benzoate complexes can be formed by nucleophilic attack of basic oxygen atoms or surface hydroxyl groups to the carbonyl group of a carbonyl compound. Benzoic acid formed during reaction may be responsible for benzoate formation on sulfated zirconia, as evidenced by the infrared spectrum of SZ(1) impregnated with 1 wt% benzoic acid (figure 8). Benzoate complexes may also originate from the acylating agent, like benzoic anhydride or benzoyl chloride, as evidenced by DRIFTS (spectra not shown in figure 8). The non-acidic ZrOH groups, which have been revealed by DRIFTS, may be involved in benzoate formation.

Two other sharp bands at 1598 and 1501 cm^{-1} indicate the presence of additional aromatic rings on the surface of the used catalysts. Comparison with the spectrum of anisole adsorbed on SZ(1) (figure 8) suggests that strongly adsorbed anisole molecules, which could not be removed by washing with CH_2Cl_2, may be accumulated on the surface. The reactant anisole coordinates *via* hydrogen-bonding of the aromatic ring to acidic OH groups and strong interaction of the oxygen atom of the methoxy group to Lewis acid sites.

In agreement with the ^{13}C-NMR measurements, no clear indication of molecularly adsorbed products or condensation products has been found by infrared spectroscopy. However, the ν(CO) vibration of the protonated ketone is expected to be covered by the ν(S=O) vibrations of the sulfate groups [39].

Finally, the spectrum of the regenerated catalyst in figure 8 demonstrates that all carbonaceous deposits can be removed by burning the used catalyst in air at 550 °C.

3.4.3. UV–Vis

Immediately after introduction of the catalyst into the reaction mixture of anisole and benzoic anhydride, a color change of all the catalysts studied into pink was observed. Figure 9 shows UV–Vis spectra of used catalysts. Stirring SZ(1) in anisole or in a solution of

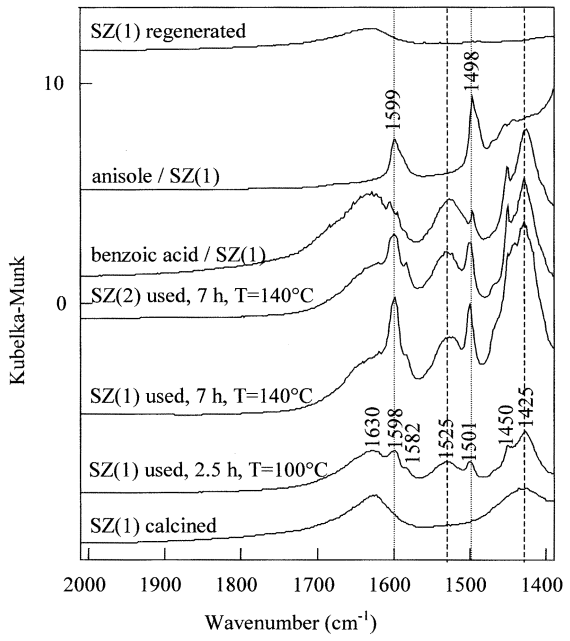

Figure 8. DRIFT spectra of SZ after calcination, use in the benzoylation of anisole, regeneration and after adsorption of reference compounds.

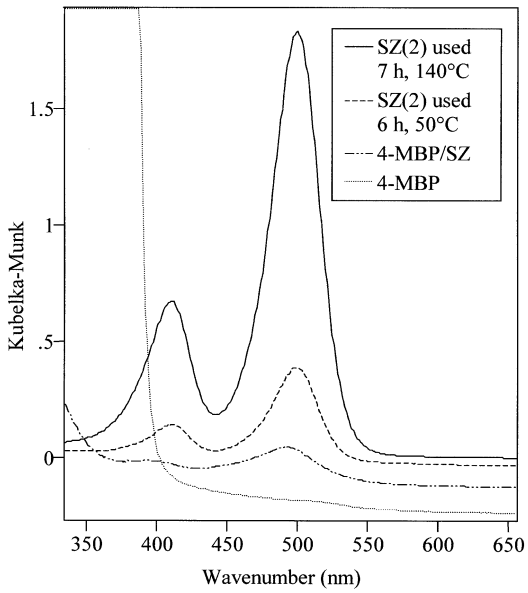

Figure 9. UV–Vis spectra of SZ after use and after adsorption of the reaction product 4-MBP.

benzoic anhydride in dichloromethane, respectively, at reaction temperature does not induce coloring. However, stirring a suspension of SZ(1) in a solution of the product 4-methoxybenzophenone in dichloromethane gives rise to the same color change as observed during the reaction. Accordingly, in the UV–Vis spectrum the same bands at 403 and 492 nm as with the used catalyst have been observed. Similar absorption spectra have been reported upon protonation of related ketones in sulfuric acid media [40] or on the surface of silica–alumina and zeolites [41]. Therefore, it is assumed that the color may be caused by the protonation of small amounts of the reaction product by acidic surface OH groups. The protonation is observed at the beginning of the reaction. At this time, the catalyst is still active. Hence, the corresponding acid sites play, probably, no crucial role as active sites in the benzoylation of anisole.

4. Summary and conclusions

Deposition of carbonaceous species has been identified as the main reason for deactivation of sulfated zirconia in the benzoylation of anisole. The catalytic activity of spent sulfated zirconia can be completely restored by burning off the deposited carbonaceous material.

The deposits consist of bidentate benzoate species. Moreover, molecules of the aromatic substrate anisole are probably strongly adsorbed on the catalyst surface. The protonated reaction product methoxybenzophenone gives rise to a coloring of the spent catalysts.

The acylating agent as well as benzoic acid formed during the reaction may be regarded as the origin of benzoate species, which may be formed under the involvement of non-acidic surface OH groups. The presence of S-free surface domains and non-acidic Zr–OH species on sulfated zirconia has been revealed by FTIR-NH_3-TPD and DRIFTS of the calcined catalysts. The mass balance of the reaction is not significantly affected by the formation of these deposits and the catalysts deactivate only moderately since the corresponding OH groups are surely not active in acylation. However, the accessibility of active sites on the used catalyst may be restricted due to steric hindrance by the bulky benzoate complexes. The population of non-acidic OH-groups on the surface of sulfated zirconia depends on the preparation method and can be minimized by applying preparation routes that ensure a more homogeneous deposition of surface sulfate species, like aerogel synthesis.

Acknowledgments

The authors wish to thank Dr. J. Radnik for XPS measurements and Mrs. K. Neitzel for performing the NH_3-TPD experiments. We are indebted to the Bundesministerium für Bildung, Wissenschaft, Forschung und Technologie (BMBF: FKZ 03C0275 and FKZ 03C0328) for financial support.

References

[1] A. Corma, Chem. Rev. 95 (1995) 559.
[2] B.M. Choudary, M. Sateesh, M.L. Kantam and K.V.R. Prasad, Appl. Catal. A 171 (1998) 155.
[3] C. deCastro, J. Primo and A. Corma, J. Mol. Catal. A 134 (1998) 215.
[4] M. Spangol, L. Gilbert, E. Benazzi and C. Marcilly, PCT Int. Appl. WO 9635, 655 (1996).
[5] K. Tanabe, T. Yamaguchi, K. Akiyama, A. Mitoh, K. Iwabuchi and K. Isogai, Proc. 8th Intern. Congr. Catal. (Verlag Chemie, Weinheim, 1984), Vol. 5, p. 601.
[6] T. Yamaguchi, T. Jin, T. Ishida and K. Tanabe, Mater. Chem. Phys. 17 (1987) 3.
[7] V. Quaschning, J. Deutsch, P. Druska, H.J. Niclas and E. Kemnitz, J. Catal. 177 (1998) 164.
[8] G.D. Yadav and A.A. Pujari, Green Chem. 1 (1999) 69.
[9] J. Deutsch, V. Quaschning, E. Kemnitz, A. Auroux, H. Ehwald and H. Lieske, Topics Catal. 13 (2000) 281.
[10] V. Quaschning, A. Auroux, J. Deutsch, H. Lieske and E. Kemnitz, J. Catal. 203 (2001) 426.
[11] D. Rohan, C. Canaff, E. Fromentin and M. Guisnet, J. Catal. 177 (1998) 296.
[12] E.G. Derouane, C.J. Dillon, D. Bethell and S.B. Derouane-Abd Hamid, J. Catal. 187 (1999) 209.
[13] U. Freese, F. Heinrich and F. Roessner, Catal. Today 49 (1999) 237.
[14] P. Moreau, A. Finiels and P. Meric, J. Mol. Catal. A 154 (2000) 185.
[15] E.G. Derouane, G. Crehan, C.J. Dillon, D. Bethell, H. He and S.B. Derouane-Abd Hamid, J. Catal. 194 (2000) 410.
[16] P. Laidlaw, D. Bethell, S.M. Brown and G.J. Hutchings, J. Mol. Catal. A 74 (2001) 187.
[17] L. Cerveny, K. Mikulcova and J. Cejka, Appl. Catal. A 223 (2002) 65.
[18] H.T. Clarke and E.J. Rahrs, Org. Synth., Coll. Vol. I, 91 (1941).
[19] T. Jin, T. Yamaguchi and K. Tanabe, J. Phys. Chem. 90 (1986) 4794.
[20] M. Bensitel, O. Saur, J.-C. Lavalley and G. Mabilon, Mater. Chem. Phys. 17 (1987) 249.
[21] M. Bensitel, O. Saur, J.-C. Lavalley and B.A. Morrow, Mater. Chem. Phys. 19 (1988) 147.
[22] V.S. Komarov and M.F. Sinilo, Kinet. Katal. 29 (1988) 701.
[23] M. Waqif, J. Bachelier, O. Saur and J.-C. Lavalley, J. Mol. Catal. 72 (1992) 127.
[24] C. Morterra, G. Cerrato and V. Bolis, Catal. Today 17 (1993) 505.
[25] A. Clearfield, G.D.P. Serrette and A.H. Khazi-Syed, Catal. Today 20 (1994) 295.
[26] L.M. Kustov, V.B. Kazansky, F. Figueras and D. Tichit, J. Catal. 150 (1994) 143.
[27] T. Riemer, D. Spielbauer, M. Hunger, G.A.H. Mekhemer and H. Knözinger, J. Chem. Soc. Chem. Commun. (1994) 1181.
[28] V. Adeeva, J.W. de Haan, J. Jänchen, G.D. Lei, V. Schünemann, L.J.M. van de Veen, W.H.M. Sachtler and R.A. van Santen, J. Catal. 151 (1995) 364.
[29] F. Babou, G. Coudurier and J.C. Vedrine, J. Catal. 152 (1995) 341.
[30] R.L.White, E.C. Sikabwe, M.A. Coelho and D.E. Resasco, J. Catal. 157 (1995) 755.
[31] E.E. Platero, M.P. Mentruit, C.O. Arean and A. Zecchina, J. Catal. 162 (1996) 268.
[32] A.A. Tsyganenko and V.N. Filiminov, J. Mol. Struct. 19 (1973) 579.

[33] F. Haase and J. Sauer, J. Amer. Chem. Soc. 120 (1998) 13503.
[34] C. Morterra, G. Cerrato, F. Pinna, M. Signoretto and G. Strukul, J. Catal. 149 (1994) 181.
[35] C. Morterra and G. Cerrato, Phys. Chem. Chem. Phys. 1 (1999) 2825.
[36] P.J. Wagner, M.A. Meador and B.-S. Park, J. Amer. Chem. Soc. 112 (1990) 5199.
[37] H.O. Kalinowski, S. Berger and S. Braun, ^{13}*C-NMR-Spektroskopie* (Georg Thieme Verlag, Stuttgart–New York, 1984) p. 285.
[38] D.D. Wirth, Tetrahedron 49 (1993) 1535.
[39] I. Ahmad, J.A. Anderson, C.H. Rochester and T.J. Dines, J. Mol. Catal. A 135 (1998) 63.
[40] R. Steward and K. Yates, J. Am. Chem. Soc. 80 (1958) 6355.
[41] B.S. Umansky and W.K. Hall, J. Catal. 124 (1990) 97.